



ELSEVIER

Available online at [www.sciencedirect.com](http://www.sciencedirect.com)

SCIENCE @ DIRECT®

PHYSICS LETTERS B

Physics Letters B 582 (2004) 187–195

[www.elsevier.com/locate/physletb](http://www.elsevier.com/locate/physletb)

# Platonic sphalerons

Burkhard Kleihaus, Jutta Kunz, Kari Myklevoll

*Institut für Physik, Universität Oldenburg, Postfach 2503, D-26111 Oldenburg, Germany*

Received 31 October 2003; received in revised form 3 December 2003; accepted 10 December 2003

Editor: T. Yanagida

## Abstract

We construct sphaleron solutions in Weinberg–Salam theory, which possess only discrete symmetries. Related to rational maps of degree  $N$ , these sphalerons carry baryon number  $Q_B = N/2$ . The energy density of these sphalerons reflects their discrete symmetries. We present an  $N = 3$  sphaleron with tetrahedral energy density, an  $N = 4$  sphaleron with cubic energy density, and an  $N = 5$  sphaleron with octahedral energy density.

© 2004 Published by Elsevier B.V. Open access under [CC BY license](https://creativecommons.org/licenses/by/4.0/).

## 1. Introduction

As observed by 't Hooft [1], the Standard Model does not absolutely conserve baryon and lepton number due to the Adler–Bell–Jackiw anomaly. In particular 't Hooft considered spontaneous fermion number violation due to instanton transitions between topologically inequivalent vacua. Manton [2] considered the possibility of fermion number violation in the weak interactions from another point of view. Showing the existence of non-contractible loops in configuration space, he predicted the existence of a static, unstable solution of the field equations, a sphaleron [3], representing the top of the energy barrier between topologically distinct vacua [4]. At finite temperature the energy barrier between distinct vacua can be over-

come due to thermal fluctuations of the fields, and vacuum to vacuum transitions can occur, accompanied by a change of baryon and lepton number. The rate for baryon number violating processes is largely determined by a Boltzmann factor, containing the height of the barrier at a given temperature, and thus by the energy of the sphaleron [5].

The non-trivial topology of configuration space of Weinberg–Salam theory gives rise to further unstable classical solutions. A superposition of sphalerons, for instance, leads to static axially symmetric solutions, multisphalerons, whose energy density is torus-like [6]. Klinkhamer, on the other hand, has constructed a static axially symmetric solution, which may be thought of as a bound sphaleron–antisphaleron system, in which sphaleron and antisphaleron are located at an equilibrium distance on the symmetry axis [7]. A conjectured generalization of these solutions [8] are static axially symmetric sphaleron–antisphaleron chains [9].

*E-mail address:* [kleihaus@marvin.physik.uni-oldenburg.de](mailto:kleihaus@marvin.physik.uni-oldenburg.de) (B. Kleihaus).

In this Letter we show, that Weinberg–Salam theory possesses a further type of classical solutions. These new solutions possess no rotational symmetry at all. Their symmetries are only discrete, and can be identified with the symmetries of platonic solids or crystals. Since these solutions are most likely unstable, we refer to them as platonic sphalerons.

Classical solutions with platonic symmetries were first observed in the Skyrme model of baryons and nuclei, where these stable soliton solutions with higher baryon number are interpreted in terms of small nuclei [10]. Solitons with platonic symmetries are also known in the Georgi–Glashow model, where they represent monopoles with higher magnetic charge [11], and they arise as skyrmion monopoles in a modified Georgi–Glashow model with higher derivative terms [12].

Monopoles with magnetic charge  $N$  and Skyrmions with baryon number  $N$  are related to rational maps of degree  $N$  [13]. In particular certain rational maps of degree  $N$  give rise to solitons with platonic symmetries [10–12]. Interestingly, the energy densities of the known classical solutions based on the same rational map but obtained in different physical models are qualitatively very similar.

We here base our construction of sphaleron solutions of Weinberg–Salam theory on rational maps of degree  $N$  as well. The rational maps then determine the behaviour of the Higgs and gauge fields at infinity. We solve the general set of static equations of motion numerically, subject to the boundary conditions specified by the rational maps. We show, that the degree  $N$  of the maps is related to the baryon number  $Q_B$  of the sphalerons:  $Q_B = N/2$ .

In particular, we here consider sphalerons based on maps with degree  $N = 1$ –5. Besides reproducing the axially symmetric sphalerons [6], we construct platonic sphalerons for  $N = 3$ –5, whose energy density has tetrahedral, cubic and octahedral symmetry, respectively. We compare the masses of the platonic sphalerons with those of the axially symmetric sphalerons, discuss the node structure of the modulus of the Higgs fields for the platonic sphalerons, and compare with the node structure of the corresponding platonic monopoles. We obtain their magnetic moments perturbatively [3], because we construct the platonic sphalerons in the limit of vanishing weak mixing angle [6,14].

## 2. Weinberg–Salam Lagrangian

We consider the bosonic sector of Weinberg–Salam theory

$$\mathcal{L} = -\frac{1}{2} \text{Tr}(F_{\mu\nu} F^{\mu\nu}) - \frac{1}{4} f_{\mu\nu} f^{\mu\nu} - (D_\mu \Phi)^\dagger (D^\mu \Phi) - \lambda \left( \Phi^\dagger \Phi - \frac{v^2}{2} \right)^2 \quad (1)$$

with SU(2) field strength tensor

$$F_{\mu\nu} = \partial_\mu V_\nu - \partial_\nu V_\mu + ig[V_\mu, V_\nu], \quad (2)$$

the SU(2) gauge potential  $V_\mu = V_\mu^a \tau_a/2$ , U(1) field strength tensor

$$f_{\mu\nu} = \partial_\mu A_\nu - \partial_\nu A_\mu, \quad (3)$$

and covariant derivative of the Higgs field

$$D_\mu \Phi = \left( \partial_\mu + igV_\mu + i\frac{g'}{2}A_\mu \right) \Phi, \quad (4)$$

where  $g$  and  $g'$  denote the SU(2) and U(1) gauge coupling constants, respectively,  $\lambda$  the strength of the Higgs self-interaction and  $v$  the vacuum expectation value of the Higgs field.

The Lagrangian (1) is invariant under local SU(2) gauge transformations  $U$ ,

$$V_\mu \rightarrow UV_\mu U^\dagger + \frac{i}{g} \partial_\mu U U^\dagger,$$

$$\Phi \rightarrow U\Phi.$$

The gauge symmetry is spontaneously broken due to the non-vanishing vacuum expectation value of the Higgs field

$$\langle \Phi \rangle = \frac{v}{\sqrt{2}} \begin{pmatrix} 0 \\ 1 \end{pmatrix}, \quad (5)$$

leading to the boson masses

$$\begin{aligned} M_W &= \frac{1}{2} g v, \\ M_Z &= \frac{1}{2} \sqrt{(g^2 + g'^2)} v, \\ M_H &= v \sqrt{2\lambda}. \end{aligned} \quad (6)$$

$\tan \theta_w = g'/g$  determines the weak mixing angle  $\theta_w$ , defining the electric charge  $e = g \sin \theta_w$ .

In Weinberg–Salam theory, baryon number is not conserved

$$\begin{aligned} \frac{dQ_B}{dt} &= \int d^3r \partial_t j_B^0 \\ &= \int d^3r \left[ \vec{\nabla} \cdot \vec{j}_B + \frac{g^2}{32\pi^2} \epsilon^{\mu\nu\rho\sigma} \text{Tr}(F_{\mu\nu} F_{\rho\sigma}) \right]. \end{aligned} \quad (7)$$

Starting at time  $t = -\infty$  at the vacuum with  $Q_B = 0$ , one obtains the baryon number of a sphaleron solution at time  $t = t_0$  [3],

$$Q_B = \int_{-\infty}^{t_0} dt \oint_S \vec{K} \cdot d\vec{S} + \int_{t=t_0} d^3r K^0, \quad (8)$$

where the  $\vec{\nabla} \cdot \vec{j}_B$  term is neglected, and the anomaly term is re-expressed in terms of the Chern–Simons current

$$K^\mu = \frac{g^2}{16\pi^2} \epsilon^{\mu\nu\rho\sigma} \text{Tr} \left( F_{\nu\rho} V_\sigma + \frac{2}{3} i g V_\nu V_\rho V_\sigma \right). \quad (9)$$

In a gauge, where asymptotically

$$V_\mu \rightarrow \frac{i}{g} \partial_\mu \hat{U} \hat{U}^\dagger, \quad \hat{U}(\infty) = 1, \quad (10)$$

$\vec{K}$  vanishes at infinity, yielding for the baryon charge of a sphaleron solution

$$Q_B = \int_{t=t_0} d^3r K^0. \quad (11)$$

Here we are interested in static classical solutions of the general field equations with vanishing time components of the gauge fields,  $V_0 = 0$  and  $A_0 = 0$ . For non-vanishing  $g'$  it is inconsistent to set the U(1) field to zero, since the U(1) current

$$j_i = -\frac{i}{2} g' (\Phi^\dagger D_i \Phi - (D_i \Phi)^\dagger \Phi) \quad (12)$$

acts as a source for the gauge potential  $A_i$ . This current also determines the magnetic moment  $\vec{\mu}$  of a classical configuration, since

$$\vec{\mu} = \frac{1}{2} \int \vec{r} \times \vec{j} d^3r. \quad (13)$$

When  $g' = 0$ , the U(1) gauge potential  $A_\mu$  decouples and may consistently be set to zero. Since we here

construct sphaleron solutions in the limit of vanishing Weinberg angle, we determine their magnetic moments only perturbatively [3]. We note, that the ratio  $\vec{\mu}/e$  remains finite for  $\theta_w \rightarrow 0$ .

### 3. Rational maps

To obtain sphaleron solutions with discrete symmetry we make use of rational maps, i.e., holomorphic functions from  $S^2 \mapsto S^2$  [13]. Treating each  $S^2$  as a Riemann sphere, the first having coordinate  $\xi$ , a rational map of degree  $N$  is a function  $R: S^2 \mapsto S^2$  where

$$R(\xi) = \frac{p(\xi)}{q(\xi)}, \quad (14)$$

and  $p$  and  $q$  are polynomials of degree at most  $N$ , where at least one of  $p$  and  $q$  must have degree precisely  $N$ , and  $p$  and  $q$  must have no common factors [13].

We recall that via stereographic projection, the complex coordinate  $\xi$  on a sphere can be identified with conventional polar coordinates by  $\xi = \tan(\theta/2) e^{i\varphi}$  [13]. Thus the point  $\xi$  corresponds to the unit vector

$$\vec{n}_\xi = \frac{1}{1 + |\xi|^2} (2\Re(\xi), 2\Im(\xi), 1 - |\xi|^2), \quad (15)$$

and the value of the rational map  $R(\xi)$  is associated with the unit vector

$$\vec{n}_R = \frac{1}{1 + |R|^2} (2\Re(R), 2\Im(R), 1 - |R|^2). \quad (16)$$

Parametrizing the Higgs field as

$$\Phi = (\Phi_0 \mathbb{1} + i \Phi_a \tau_a) \frac{v}{\sqrt{2}} \begin{pmatrix} 0 \\ 1 \end{pmatrix}, \quad (17)$$

we impose at infinity the boundary conditions

$$\Phi_0 = 0, \quad \Phi_a \tau_a = (\vec{n}_R) \cdot \vec{\tau} =: \tau_R. \quad (18)$$

The boundary conditions for the gauge field are obtained from the requirement  $D_i \Phi = 0$  at infinity, yielding

$$V_i = \frac{i}{g} (\partial_i \tau_R) \tau_R, \quad (19)$$

i.e., the gauge field tends to a pure gauge at infinity,  $V_i = \frac{i}{g} (\partial_i U_\infty) U_\infty^\dagger$ , with  $U_\infty = i \tau_R$ .

Subject to these boundary conditions, and the gauge condition

$$\partial_i V^i = 0, \quad (20)$$

we then solve the general set of field equations, involving 4 functions  $\Phi_0(x, y, z)$ ,  $\Phi_a(x, y, z)$  for the Higgs field and 9 functions  $V_i^a(x, y, z)$  for the gauge field, and  $V_0^a = 0$ . The solutions additionally satisfy the condition  $\partial^\mu \text{Tr}(V_\mu \Phi) = 0$ , corresponding to  $\Phi_0(x, y, z) = 0$ .

We here consider platonic sphalerons obtained from maps  $R_N$ ,

$$R_3(\xi) = \frac{\sqrt{3}a\xi^2 - 1}{\xi(\xi^2 - \sqrt{3}a)}, \quad a = \pm i, \quad (21)$$

$$R_4(\xi) = c \frac{\xi^4 + 2\sqrt{3}i\xi^2 + 1}{\xi^4 - 2\sqrt{3}i\xi^2 + 1}, \quad c = 1, \quad (22)$$

$$R_5(\xi) = \frac{\xi(\xi^4 + b\xi^2 + a)}{a\xi^4 - b\xi^2 + 1}, \quad b = 0, a = -5. \quad (23)$$

Note, that the choice  $a = 0$  in (21), and  $a = b = 0$  in (23) yields the axially symmetric sphalerons of Ref. [6] for  $N = 3$  and  $N = 5$ , respectively, in a different gauge, while the axially symmetric sphaleron for  $N = 4$  is obtained from  $R_4(\xi) = \xi^4$ .

The baryon number  $Q_B$  of the sphalerons is obtained from Eq. (11), after performing a gauge transformation with

$$U = \exp(-i\Omega(x, y, z)\tau_R/2), \quad (24)$$

where  $\Omega$  tends to  $\pi$  at infinity and vanishes at the origin. We note, that the non-gauge transformed Chern–Simons density  $K^0$  vanishes identically for the spherically and axially symmetric sphalerons, due to the ansatz of the gauge potential.<sup>1</sup> In contrast, for the platonic sphalerons the non-gauge transformed Chern–Simons density  $K^0$  is non-trivial, and we checked numerically that it does not contribute to the baryon number for the platonic sphalerons. Thus the only contribution arises from the gauge transformation  $U$ , Eq. (24). Consequently, the platonic sphalerons have baryon number

$$Q_B = \frac{N}{2}. \quad (25)$$

<sup>1</sup> Note that for the bisphalerons of [16]  $K^0$  does not vanish and contributes to the baryon number.

#### 4. Platonic sphalerons

To construct platonic sphalerons, we transform to dimensionless coordinates  $\tilde{x} = xvg$ ,  $\tilde{y} = yvg$ ,  $\tilde{z} = zvg$ , and scale the gauge potential  $V_\mu \rightarrow vV_\mu$ . The set of classical equations of motion is then solved numerically, subject to the boundary conditions specified by (18), (19) for the rational maps (21)–(23). We employ the Gauß–Seidel algorithm on an equidistant mesh in the coordinates  $(\tilde{x}, \tilde{y}, \tilde{z})$  defined by

$$\begin{aligned} \tilde{x} &= R_L \frac{\sin \tilde{x}}{\cos^2 \tilde{x}} \frac{\cos^2 \alpha}{\sin \alpha}, \\ \tilde{y} &= R_L \frac{\sin \tilde{y}}{\cos^2 \tilde{y}} \frac{\cos^2 \alpha}{\sin \alpha}, \\ \tilde{z} &= R_L \frac{\sin \tilde{z}}{\cos^2 \tilde{z}} \frac{\cos^2 \alpha}{\sin \alpha}, \end{aligned} \quad (26)$$

where  $R_L$  defines the extend of the integration volume and  $\alpha < \pi/2$  defines the range  $[-\alpha, \alpha]$  of the coordinates  $\tilde{x}$ ,  $\tilde{y}$ ,  $\tilde{z}$ . The numerical solutions are obtained with  $\alpha = 1.082$  and  $R_L = 12$  for  $N = 3$  and  $R_L = 15$  for  $N = 4, 5$ . The mesh consists of 71 meshpoints in each direction. The numerical solutions for the field components are smooth.

The numerical solutions also satisfy the relation among the energy contributions

$$\begin{aligned} \int \frac{1}{2} \text{Tr}(F_{\mu\nu} F^{\mu\nu}) d^3r &= \int (D_\mu \Phi)^\dagger (D^\mu \Phi) d^3r \\ &+ 3\lambda \int \left( \Phi^\dagger \Phi - \frac{v^2}{2} \right)^2 d^3r, \end{aligned} \quad (27)$$

obtained from a scaling argument, with an accuracy of  $10^{-2}$ .  $\Phi_0(x, y, z) = 0$  within the numerical accuracy.

Turning to the numerical results, we first address the energy density of the platonic sphalerons. Defining the energy density  $\varepsilon$  by

$$M = \frac{1}{4\pi} \int \varepsilon(\vec{x}) dx dy dz, \quad (28)$$

where  $M$  is the mass in units of  $4\pi v/g$ , we present surfaces of constant energy density  $\varepsilon$  in Fig. 1 for the platonic sphalerons based on the maps (21), (22), and (23), for  $M_H = M_W$ . The energy density of these sphalerons clearly exhibits tetrahedral, cubic and octahedral symmetry, respectively. Since the energy

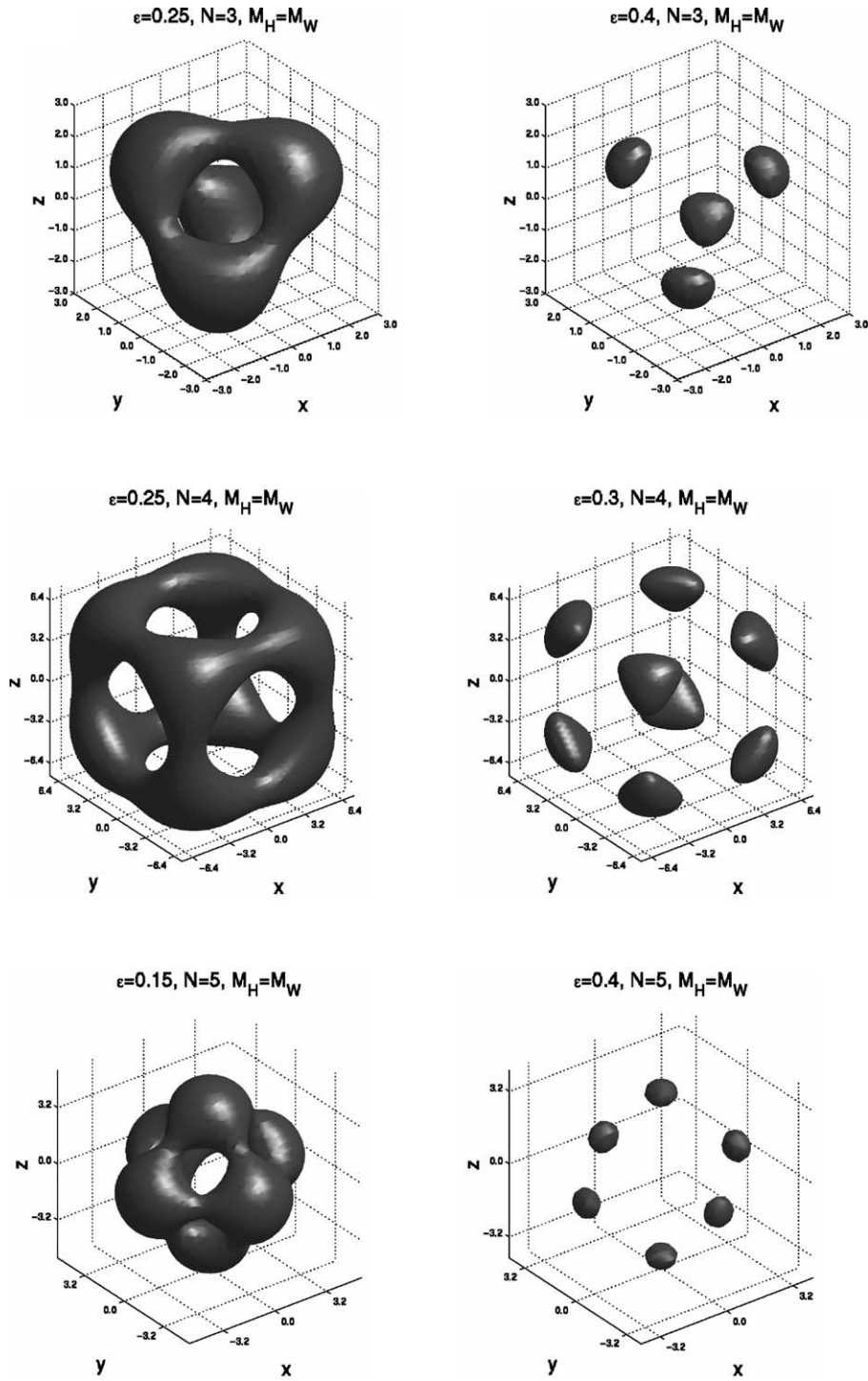


Fig. 1. Surfaces of constant energy density  $\epsilon$  are shown for the tetrahedral sphaleron ( $N = 3$ ), the cubic sphaleron ( $N = 4$ ), and the octahedral sphaleron ( $N = 5$ ).

Table 1

The masses  $M(N)$  of sphaleron solutions based on maps of degree  $N = 1-5$  are presented in units of  $4\pi v/g$  for  $M_H = M_W$  and  $M_H = 2M_W$ , together with the mass ratios  $(M(N)/NM(1))$ .  $N^*$  configurations represent axially symmetric sphalerons. Also shown are the magnetic moments  $\mu$  in units of  $2\pi g'/(3g^3v)$  and the magnetic moment ratios  $(\mu(N)/N\mu(1))$

$N$	$M(N) [4\pi v/g] (M(N)/NM(1))$		$\mu(N) [2\pi g'/(3g^3v)] (\mu(N)/N\mu(1))$	
	$M_H = M_W$	$M_H = 2M_W$	$M_H = M_W$	$M_H = 2M_W$
1	1.82 (1.00)	1.98 (1.00)	21.12 (1.00)	19.18 (1.00)
2*	3.60 (0.99)	4.03 (1.02)	44.3 (1.05)	38.9 (1.01)
3	5.33 (0.98)	6.09 (1.03)	24.1 (0.38)	22.0 (0.38)
3*	5.44 (1.00)	6.19 (1.04)	70.7 (1.12)	60.9 (1.06)
4	7.07 (0.97)	8.19 (1.04)	0. (0.)	0. (0.)
4*	7.34 (1.01)	8.46 (1.07)	100.2 (1.19)	84.2 (1.10)
5	8.90 (0.98)	10.36 (1.05)	39.0 (0.37)	35.2 (0.37)
5*	9.30 (1.02)	10.83 (1.10)	132.2 (1.25)	110.0 (1.15)

density of a platonic sphaleron is qualitatively very similar to the energy density of a platonic monopole and a platonic Skymion obtained from the same map [13], this indicates, that the shape of the energy density of a classical solution is determined primarily by the rational map, and rather independent of the model and the stability of the solution.

In Table 1 we present the masses of these platonic sphalerons with  $N = 3-5$  in units of  $4\pi v/g$  for two values of the Higgs mass,  $M_H = M_W$  and  $M_H = 2M_W$ . Also exhibited are the masses of the axially symmetric sphalerons [6] with winding number  $N = 2-5$ ,  $N = 1$  represents the spherically symmetric sphaleron [3]. For the Higgs masses considered, the mass  $M(N)$  of the platonic sphalerons is slightly smaller than the mass of the corresponding axially symmetric sphalerons. (We note, that the mass difference is significantly larger than the numerical error for the masses.) Likewise, the mass of platonic Skyrmons is smaller than the mass of the corresponding axially symmetric Skyrmons [10]. In contrast, the mass of platonic skyrmion monopoles is slightly higher than the mass of the corresponding axially symmetric skyrmion monopoles [12]. Comparing the mass  $M(N)$  of the platonic sphalerons with  $N$  times the mass  $M(1)$  of the spherically symmetric sphaleron, we observe, that for the Higgs masses considered here, their ratio  $M(N)/NM(1)$  is close to one. (For axially symmetric sphalerons, the mass ratio  $M(N)/NM(1)$  is smaller than one for small Higgs masses and larger than one for large Higgs masses [6].)

We next address the modulus of the Higgs field, and in particular, the location of its nodes. All sphalerons possess a node at the origin, which is the only

node for the spherically symmetric sphaleron [3] and the axially symmetric sphalerons [6]. For the platonic sphalerons we expect a pattern of nodes, in accordance with the symmetries of the solutions. For the tetrahedral sphaleron ( $N = 3$ ), for instance, four ( $N + 1$ ) additional nodes may be located along the four spatial diagonals, which pass through the maxima of the energy density. Alternatively, four additional nodes could be located at the centers of the faces of the tetrahedron.

In Fig. 2 we exhibit the components of the Higgs field  $\Phi_a$ ,  $a = 1, 2, 3$ , in units of  $v/\sqrt{2}$  along those spatial directions, where in accordance with the symmetries of the platonic sphalerons nodes of the modulus of the Higgs field may be found. At a node of the modulus of the Higgs field all components must vanish. As seen in Fig. 2(a), (b), the modulus of the Higgs field of the tetrahedral sphaleron has indeed five nodes, four located on the diagonals close to the maxima of the energy density, and one located at the origin. One may thus be tempted to interpret the tetrahedral sphaleron as a superposition of four sphalerons ( $N = 1$ ) located at the nodes along spatial diagonals and one antisphaleron ( $N = -1$ ) located at the origin. The energy density at the origin is small however.

Similarly, we observe seven nodes for the modulus of the Higgs field of the octahedral sphaleron ( $N = 5$ ), as seen in Fig. 2(c). In accordance with the symmetries, one node is located at the origin, and six ( $N + 1$ ) nodes are located symmetrically on the Cartesian axes. Again these six nodes are associated with the six maxima of the energy density, suggesting to interpret the octahedral sphaleron as a superposition of six sphalerons ( $N = 1$ ) and one antisphaleron

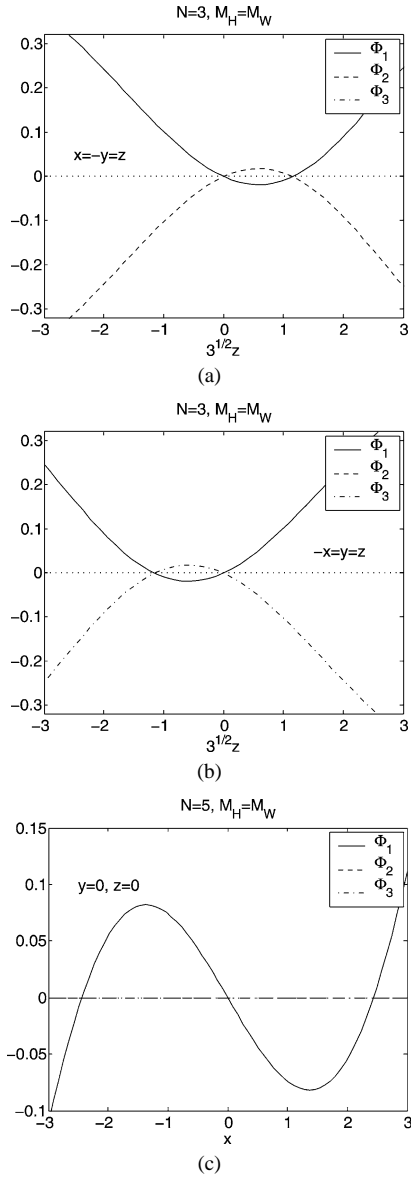


Fig. 2. The components of the Higgs field  $\Phi_a$ ,  $a = 1, 2, 3$ , are shown (in units of  $v/\sqrt{2}$ ) for the tetrahedral sphaleron ( $N = 3$ ) along the diagonals  $x = -y = z$  (a) and  $-x = y = z$  (b) (in dimensionless coordinates  $x, y, z$ ). In (a)  $\Phi_3 = \Phi_1$ , and in (b)  $\Phi_2 = \Phi_1$ . Along the diagonal  $x = y = z$  all three components coincide with the component  $\Phi_3$  of (b), while along the diagonal  $-x = -y = z$   $\Phi_1$  coincides with the component  $\Phi_2$  of (a), and  $\Phi_2 = \Phi_3$  coincides with  $\Phi_1$  of (a).

For the octahedral sphaleron ( $N = 5$ ) the components of the Higgs field  $\Phi_a$  are shown along the Cartesian  $x$ -axis (c). Here  $\Phi_2 = \Phi_3 = 0$ . Along the  $y$ -axis  $\Phi_1 = \Phi_3 = 0$  and  $\Phi_2$  coincides with  $\Phi_1$  of (c), while along the  $z$ -axis  $\Phi_1 = \Phi_2 = 0$  and  $\Phi_3$  coincides with  $\Phi_1$  of (c).

( $N = -1$ ), although the energy density at the central node is small. In contrast to the  $N + 2$  nodes of the tetrahedral and octahedral sphalerons, we observe only a single node for the cubic sphaleron ( $N = 4$ ). There are no nodes along the spatial diagonals close to the eight ( $N + 3$ ) maxima of the energy density, which would be required for an interpretation of the cubic sphaleron in terms of a superposition of sphalerons ( $N = 1$ ) and antisphalerons, and there are no nodes along the Cartesian axes as well.

Comparing the node structure of the platonic sphalerons with the node structure of the platonic monopoles, we note, that they are completely analogous for the rational maps considered [13]. Associating for the monopoles a node of the Higgs modulus with the location of a magnetic charge, an  $N = 3$  tetrahedral monopole, for instance, would then be composed of four monopoles and one antimonopole, and thus possess the proper total magnetic charge [15].

In Table 1 we also exhibit the magnetic moment  $\mu$  in units of  $2\pi g'/(3g^3 v)$  of the platonic and axially symmetric sphalerons [6]. The magnetic moment is obtained perturbatively, since the sphaleron solutions are constructed in the limit of vanishing weak mixing angle. (For the axially symmetric sphalerons the deviation of the perturbative value of  $\mu$  from the non-perturbative value [6] is only 1% for  $\theta_w = 0.5$  and  $M_H = M_W$ .) The magnetic moment  $\mu(N)$  of the axially symmetric sphalerons increases strongly with  $N$ , yielding a ratio  $\mu(N)/N\mu(1)$  on the order of one. The magnetic moment  $\mu(N)$  of the corresponding platonic sphalerons is considerably smaller, yielding a ratio  $\mu(N)/N\mu(1)$  of only about one third for  $N = 3$  and  $N = 5$ , while the magnetic moment of the  $N = 4$  platonic sphaleron vanishes (within numerical accuracy:  $\mu < 10^{-3}$ ).

## 5. Conclusions

We have constructed sphalerons in Weinberg–Salam theory which possess only discrete symmetries. These sphalerons are based on rational maps of degree  $N$  and have baryon number  $Q_B = N/2$ . The energy density of the platonic sphalerons constructed for  $N = 3$ –5 possesses tetrahedral, cubic and octahedral symmetry. Interestingly, the energy densities of platonic sphalerons are qualitatively very similar to the

energy densities of platonic monopoles and platonic Skyrmions, obtained from the same rational map [12, 13]. We thus conclude, that the shape of the energy density of a classical solution is determined primarily by the rational map, and rather independent of the model and the stability of the solution.

The mass  $M(N)$  of the platonic sphalerons is lower than the mass of the corresponding axially symmetric sphalerons, for the Higgs masses considered, and their mass ratio  $M(N)/NM(1)$  is close to one. For Skyrmions, monopoles and skyrmed monopoles a second map with degree  $N = 5$  has been considered, leading to solutions with dihedral symmetry [12, 13]. The dihedral Skyrmion and skyrmed monopole possess a slightly smaller mass than their octahedral counterparts [12, 13]. We expect a dihedral sphaleron ( $N = 5$ ) in Weinberg–Salam theory as well, and also platonic sphalerons based on maps of higher degree  $N > 5$ .

The node structure of the modulus of the Higgs field of the platonic sphalerons and of the platonic monopoles is also completely analogous for the rational maps considered. The tetrahedral sphaleron has five nodes, four located on the diagonals close to the maxima of the energy density, and one located at the origin. Similarly, the octahedral sphaleron has seven nodes, six located symmetrically on the Cartesian axes close to the maxima of the energy density, and one located at the origin. The cubic sphaleron, in contrast, has a single node located at the origin.

The perturbatively obtained magnetic moments of the platonic sphalerons do not exhibit the (almost) linear growth with  $N$ , observed for the axially symmetric sphalerons [6]. The magnetic moments of the tetrahedral and octahedral sphalerons are only about one third of the magnetic moments of the corresponding axially symmetric sphalerons, and the magnetic moment of the cubic sphaleron vanishes. The influence of a finite mixing angle on the magnetic moment and on the masses is expected to be small [6], and will be considered elsewhere.

The solutions constructed here possess an additional property, they satisfy  $\partial^\mu \text{Tr } V_\mu \Phi = 0$ , corresponding to  $\Phi_0(x, y, z) = 0$ . Thus only three of the four Higgs field functions are non-trivial. Without this symmetry property more general solutions may be found. In the case of spherical symmetry, for instance, additional unstable solutions, bisphalerons, ap-

pear [16]. Their generalization to axial symmetry and platonic symmetries remains open.

We conclude from our results, that the occurrence of localized finite energy solutions with platonic symmetries is a more general phenomenon than previously thought, since it appears to be present in various non-Abelian field theories. In particular, since the solutions constructed here are most likely unstable, and thus sphalerons, stability is not needed for such solutions to exist. Consequently, we expect the presence of platonic sphalerons in further theories, such as pure Yang–Mills theory coupled to gravity [17].

## Acknowledgements

B.K. gratefully acknowledges support by the DFG under contract KU612/9-1, and K.M. by the Research Council of Norway under contract 153589/432.

## References

- [1] G. 't Hooft, Phys. Rev. Lett. 37 (1976) 8.
- [2] N.S. Manton, Phys. Rev. D 28 (1983) 2019.
- [3] F.R. Klinkhamer, N.S. Manton, Phys. Rev. D 30 (1984) 2212.
- [4] T. Akiba, H. Kikuchi, T. Yanagida, Phys. Rev. D 38 (1988) 1937.
- [5] L.D. McLerran, Acta Phys. Pol. B 25 (1994) 309;  
V.A. Rubakov, M.E. Shaposhnikov, Usp. Fiz. Nauk 166 (1996) 493 (in Russian), Phys. Usp. 39 (1996) 461;  
F.R. Klinkhamer, C. Rupp, J. Math. Phys. 44 (2003) 3619;  
K. Enqvist, A. Mazumdar, Phys. Rep. 380 (2003) 99;  
M. Dine, A. Kusenko, hep-ph/0303065.
- [6] B. Kleihaus, J. Kunz, Phys. Lett. B 329 (1994) 61;  
B. Kleihaus, J. Kunz, Phys. Rev. D 50 (1994) 5343.
- [7] F.R. Klinkhamer, Nucl. Phys. B 410 (1993) 343.
- [8] Y. Brihaye, J. Kunz, Phys. Rev. D 50 (1994) 4175.
- [9] B. Kleihaus, J. Kunz, Y. Shnir, Phys. Lett. B 570 (2003) 237;  
B. Kleihaus, J. Kunz, Y. Shnir, Phys. Rev. D 68 (2003) (R), in press.
- [10] E. Braaten, S. Townsend, L. Carson, Phys. Lett. B 235 (1990) 147;  
R.A. Battye, P.M. Sutcliffe, Phys. Rev. Lett. 79 (1997) 363;  
R.A. Battye, P.M. Sutcliffe, Phys. Lett. B 416 (1998) 385.
- [11] N.J. Hitchin, N.S. Manton, M.K. Murray, Nonlinearity 8 (1995) 661;  
C.J. Houghton, P.M. Sutcliffe, Commun. Math. Phys. 180 (1996) 343;  
C.J. Houghton, P.M. Sutcliffe, Nonlinearity 9 (1996) 385;  
P.M. Sutcliffe, Int. J. Mod. Phys. A 12 (1997) 4663.
- [12] D.Yu. Grigoriev, P.M. Sutcliffe, D.H. Tchrakian, Phys. Lett. B 540 (2002) 146.



- [13] C.J. Houghton, N.S. Manton, P.M. Sutcliffe, Nucl. Phys. B 510 (1998) 507.
- [14] B. Kleihaus, J. Kunz, Y. Brihaye, Phys. Lett. B 273 (1991) 100; J. Kunz, B. Kleihaus, Y. Brihaye, Phys. Rev. D 46 (1992) 3587.
- [15] P.M. Sutcliffe, Phys. Lett. B 376 (1996) 103.
- [16] J. Kunz, Y. Brihaye, Phys. Lett. B 216 (1989) 353; L. Yaffe, Phys. Rev. D 40 (1989) 3463.
- [17] R. Bartnik, J. McKinnon, Phys. Rev. Lett. 61 (1988) 141; B. Kleihaus, J. Kunz, Phys. Rev. Lett. 78 (1997) 2527.